Application of remote monitoring and ground-based sensing in pastoralism

S. Oleinik, *V.* Skripkin, *T.* Lesnyak*, and *D.* Litvin

Federal State Budgetary Educational Institution of Higher Education «Stavropol State Agrarian University» 355000, Stavropol, Russia

Abstract. The development and implementation of an innovative system applying digital aerospace technologies in pastoralism constitute one of the current trends in agricultural development designed to solve numerous problems associated with soil fertility restoration in grazing pastures. Here, a promising line of research is to explore the feasibility of using satellite systems for an overall nutrient yield assessment per hectare of grazing land. The present article describes a comprehensive approach to the optimization of pastoralism that is based on remote methods for assessing pasture fertility using unmanned aerial vehicles (UAVs) and artificial Earth satellites. An analysis of existing methodological approaches reveals that the formalization of prediction processes is complicated by the lack of a theoretical basis for creating appropriate model-algorithmic support. The data on vegetation index dynamics and the nutritional values of forage plants obtained by interpreting imagery from a UAV camera and the multispectral cameras of a satellite service, as well as data from a portable handheld nitrogen sensor, were compared with the actual nutritional values of pasture plants. The study results provide a means to optimize the grouping of grazing animals, taking into account the actual possibility of achieving an increase in live weight. The provided findings indicate the possibility of achieving an additional 11.06% increase in daily live weight gain in young sheep (Jalgin Merino) when keeping them in pasture areas having a vegetation index of at least 0.5. Remote monitoring based on satellite service allows more efficient use of pastures. Study shows a positive relationship between remote sensing NDVI and feed nutritional value. Animal grazing optimization provides an additional 11.06% increase in live weight gain.

1 Introduction

The development and implementation of innovative agricultural production technologies in pastoralism aimed at achieving the fifth and sixth technological paradigms involve the use of remote methods for monitoring production processes, the most developed of which employ unmanned aerial vehicles (UAVs), space satellite systems, monitoring of air parameters, etc [44, 39].

* Corresponding author: tatastav026@gmail.com

In order to justify the structure of the system for monitoring the state of forage crops in cultivated pastures on the basis of remote sensing data, it is necessary to perform all procedures as per the algorithm of the assessment problem. The algorithm can only be implemented when an electronic digital map of the field is generated. In this case, the surface area of the field is virtually (on an electronic map) divided into elementary sections of a given spatial discreteness [26, 27, 3].

A modern, innovative approach to the development of animal husbandry should provide high end-result predictability, information support in making informed managerial decisions, reduction in weighted average risks, and, ultimately, increased labor productivity, which is of great importance in agriculture [44, 40].

Data on the state parameters of forage phytomass can be used to identify pasture degradation areas and areas of dry grass, as well as to track and monitor the movement of livestock along paddock ks [36].

Modern information-measurement systems for aerospace monitoring of pastures, as well as associated information technologies, require further improvement of predictive mathematical models of both pasture productivity and the productive qualities of grazing animals [32, 16].

For example, the Chinese *High-Resolution Earth Observation Systems* are successfully implemented in China obtaining excellent high-resolution remote sensing images (GF series), i.e., of the same or even higher quality in terms of scanning width, spatial resolution, and revisit period than similar foreign satellite imagery [41, 45, 35, 2].

According to Shuang Li et al., satellite-derived NDVI (Normalized Difference Vegetation Index) data are widely used to analyze vegetation dynamics and its relationship to climate extremes [20].

However, Xiangyi Li et al. argue that the amount of data increasing on regional and global scales indicates a complex and heterogeneous relationship between the NDVI and climate variability due to differences in the characteristics of plant biomass. For example, Sergio Vicente-Serrano et al. show that vegetation is affected by droughts worldwide, while Qiang Zhang et al. report positive effects of drought on vegetation in most regions of China [21, 42, 37, 40, 4, 10].

Given that the issue associated with using remote methods for assessing the quality of pasture areas is not yet fully understood, thus leaving room for debate, the present article aims to study the relationship of vegetation indices obtained using the methods of remote digital aerospace technologies with the grazing capacity of pastures and the live weight of sheep.

2 Materials and methods

In order to achieve the specified aim, we studied the pasture areas of a breeding farm used in the breeding and rearing of fine-wool Jalgin Merino sheep. This farm is located in an arid region of Stavropol Territory in the south of Russia.

2.1 Climatic conditions

On the territory of the farm, the climate is distinctly continental with temperatures ranging from the minimum of −34°C in winter up to the maximum of +42°C in summer. Average annual precipitation amounts to 320–412 mm increasing from northeast to southwest.

The farm is located in an arid area where summers are long, hot, and dry with an average July temperature of +28 °C. Despite frequent frosts, autumn is warm and long. In summer, an east wind carries hot air from Central Asian deserts, which results in droughts

and dust storms occurring at wind speeds of 15–20 m/s. Droughts and hot dry winds of varying intensity are typical for the pastures of southern Russia, with 85–100 dry days observed each summer.

2.2 Data collection and processing

Multispectral images from Copernicus Sentinel-2 remote sensing satellites of the European Space Agency (European Space Agency) were used as objectively observable data on the current state of pastures.

The set of data constitutes a by-product of data editing conducted by the National Geospatial-Intelligence Agency (NGA) to obtain the final Shuttle Radar Topographic Mission (SRTM) data (DTED® 2). The data have been edited to map water bodies satisfying the minimum capture criteria, such as oceans, lakes, and watercourses. Ocean elevations were set to zero, while lake elevations were set to a constant value. The elevations of water surfaces (e.g., lakes) were constant. Rivers were monotonically stepped down in order to maintain proper flow. The data were edited on the basis of matrices having a resolution of 30 m. The coordinate system for data was used in accordance with the World Geodetic System (WGS) 84, i.e., the generally accepted Earth-fixed global astro-geodetic and gravimetric reference frame. Horizontal and vertical accuracy values amounted to 20 m (90%) and 16 m (90%), respectively.

The studies used files in the PLY format (Polygon Model File), i.e., a format that is known as the Stanford Triangle Format or the Polygon File Format primarily developed to store three-dimensional data from 3D scanners. The format supports a relatively simple object description in the form of a list of flat polygons. Moreover, PLY can store various object properties, including color and transparency, texture coordinates, surface normals, etc. This format allows for different properties of the front and back of a polygon [45].

In the present work, we studied the Normalized Difference Vegetation Index (NDVI), i. e., a standardized index indicating the presence and state of green vegetation (relative biomass). The specified index employs the contrast of characteristics between red and near-infrared (NIR) bands from a multispectral raster dataset: chlorophyll pigment absorption and high vegetation reflectance, respectively.

NDVI is determined as follows:

$$NDVI = (NIR - R)/(NIR + R) \quad (1)$$

In order to determine the moisture content, the Normalized Difference Moisture Index (NDMI) was used, which is sensitive to moisture levels in vegetation. This index used to monitor droughts and fuel levels in fire-prone areas employs NIR and SWIR bands to produce a ratio intended to mitigate the effects of illumination and atmosphere.

NDMI is determined by the formula:

$$NDMI = \frac{NIR - SWIR1}{NIR + SWIR1} \quad (2)$$

Also of interest is the study of the Soil-Adjusted Vegetation Index (SAVI), which attempts to minimize the effect of soil brightness using a soil brightness correction factor. It is often applied to desert areas exhibiting a lack of vegetation, with values ranging from −1.0 to 1.0. This index is determined as follows:

$$SAVI = \left(\frac{NIR - RED}{NIR + RED + L}\right) * (1 + L) \quad (3)$$

2.3 Formation of experimental animal groups

In order to determine the effect of pasture forages characterized by different vegetation indices on the productive qualities of animals, two groups of Jalgin Merino sheep were formed.

All animals for the study were selected from young sheep in fattening by identifying relatively similar pairs of animals for the compared groups. The first group of sheep was grazed on a pasture whose NDVI varied from 0.5 to 0.6, while the second group was grazed on a pasture having an index of 0.3–0.35.

The number of young (6-month-old) sheep in fattening in each group amounted to 20. The selected animals were kept under observation for 60 days, during which period the live weight of animals was determined by means of a livestock scale having an accuracy of ±0.10 kg.

The formed groups of sheep were grazed on pastures primarily comprising legumes and grasses (25:75%): *Onobrychis arenaria*, *Medicago falcata*, *Festuca pratensis*, and *Lolium perenne*.

2.4 Zootechnical analysis of forages

In order to validate data obtained using a remote method, vegetation samples were collected from pasture areas via the contact method to be subjected to a zootechnical analysis in the laboratory. Sampled during the main vegetation period (June–July), pasture forages were studied using standard laboratory methods. The chemical composition of forages (crude protein, crude fiber, crude fat, crude ash, calcium, phosphorus, and amino acid composition) and moisture content were determined using the equipment of such companies as INGOS (Czech Republic), FIBRETHERM (Germany), and VELP SCIENTIFICA (Italy) at a specialized accredited laboratory Feed and Metabolism of the Stavropol State Agrarian University (Certificate of Accreditation No. ROSS RU.0001.21PU12 of 10/28/2014).

Free amino acids in forages (sum of cystine and cysteine; methionine; lysine; threonine; alanine; aspartic acid; glutamic acid; glycine; histidine; isoleucine; leucine; phenylalanine; proline; serine; tyrosine; valine) were determined via extraction in dilute hydrochloric acid. Nitrogenous macromolecules extracted together with amino acids were precipitated using sulfosalicylic acid to be filtered out. To this end, the acidity of the filter medium was brought to 2.20 pH. The amino acids were separated using ion exchange chromatography; then, a reaction with ninhydrin was used to determine their concentrations via photometric detection at a wavelength of 570 nm. The total content (sum of free and bound forms) of individual amino acids was ascertained via hydrolysis depending on the individual amino acids to be determined. Prior to hydrolysis, cystine (cysteine) and methionine were oxidized to cysteic acid and methionine sulfone, respectively. The tyrosine content was determined in the hydrolysates of unoxidized samples. All the other amino acids specified above were detected in both oxidized and unoxidized samples. Oxidation was carried out at 0°C in a mixture of performic acid and phenol. The excess oxidant was decomposed with sodium disulfide. Oxidized or unoxidized samples were subjected to hydrolysis in hydrochloric acid having a molar concentration of 6 mol/dm for 23 h. The acidity of the hydrolysate medium was brought to 2.20 pH. The amino acids were separated using ion exchange chromatography and derivatized with ninhydrin to be detected at a wavelength of 570 nm (440 nm for proline).

The obtained data were processed using IBM SPSS Statistics 26 software.

3 Results

Field contours are estimated and refined according to remote sensing data (panchromatic, color, and multispectral Earth surface images) using a program for automatic interpretation and vectorization. Following processing, the raster orthomosaic is converted into a set of vector linear objects, i. e., field contours. In addition to topographic interpretation, multispectral classification can be carried out. For these purposes, it is possible to use statistical and texture characteristics in any raster band or virtual bands, drawing on the formula for NDVI.

3.1 Construction of a 3D model of the considered pasture area

The geographic coordinates of points (in other words, spatial data components) can serve as another effective predictor of forage biomass productivity [9, 5].

Figure 1 presents a digital elevation model, i.e., a representation of elevations, in which darker areas correspond to lower elevations relative to the reference (e.g., sea level), while light areas correspond to hills and high ground. The present figure exhibits a low spatial resolution, i.e., large rectangles indicating elevations.

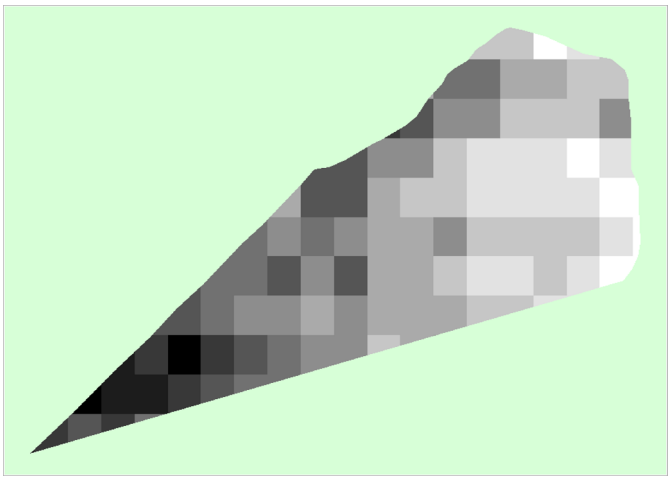

Fig. 1. Color interpretation of elevations (cell width in meters)

To build a 3D model of the pasture under study, these data comprise the longitude (degrees), latitude (degrees), and elevation (m) of the considered pasture area.

The accompanying SRTM Water Body Data (SWBD) are distributed in separate layers in the 3D Shapefile format, i.e., containing data on the elevation coordinate.

Several scientists note that the application of image-based modeling process using SfM algorithms, which is particularly common in “classical topics for photogrammetry,” is also becoming increasingly widespread in such fields as forestry and agriculture [23, 33, 13, 1, 28].

Digital photogrammetry paired with multi-view stereo algorithms using computer vision has significantly improved the acquisition of data on the state of plant biomass.

The obtained space imagery helped to construct a 3D model of the pasture under study. This model enables the estimation of surface topography, moisture accumulation, as well as the accumulation forage and pasture plant biomass.

The Earth Observation-based Anomaly Detection (EOAD) approach presented in an article by Liliana Castillo-Villamor et al. was able to map plot-level anomalies in rice crops in Colombia, while providing a plan for their elimination [5].

In a study by Yang Liu, Hongxing Liu, et al. a new method was presented combining object-based image analysis and DEM-based stream network analysis to map and quantify lentic habitats with the use of readily available ESA Sentinel-2 multispectral images and USGS DEMs. This integrated method was applied to the entire Mobile River Basin (USA), with lentic habitats at the basin scale delineated and inventoried at a spatial resolution of 10 m [23].

Multispectral and hyperspectral imaging technologies have become powerful tools in detecting and monitoring vegetation along with their productivity indices. These technologies provide both spatial and spectral information about vegetation, with the spectral region spanning wavelengths from 400 to 2500 nm [14, 7, 21].

Despite a considerable amount of current research on the quality of vegetation cover for grazing animals, namely the impact of vegetation quality on their productivity, this issue remains understudied.

3.2 Representativeness of the main vegetation indices

Given the NDVI consistency with the drought index classification, several scientists demonstrated the effectiveness of NDVI application [30, 31, 6, 24].

German scientists primarily focused their research on the field observations of aboveground pasture biomass, since it is problematic to monitor the quality of vegetation cover on a large scale in terms of time and labor intensity. In this connection, it seems relevant to apply remote methods for studying the vegetation index. One of these involves the use of satellite surveillance systems providing data over the required period while enabling lower labor-intensity [18].

A satellite image of the Stavropol Territory (26th district) serves as an example showing a surface colored according to the vegetation index scale (NDVI).

In order to identify pasture areas having preferred and stunted vegetation, a multispectral camera was used to perform a survey, followed by the construction of a NDVI-based surface. Areas exhibiting the lowest NDVI value indicate stunted vegetation or plants having damaged leaves (Figs. 2 and 2).

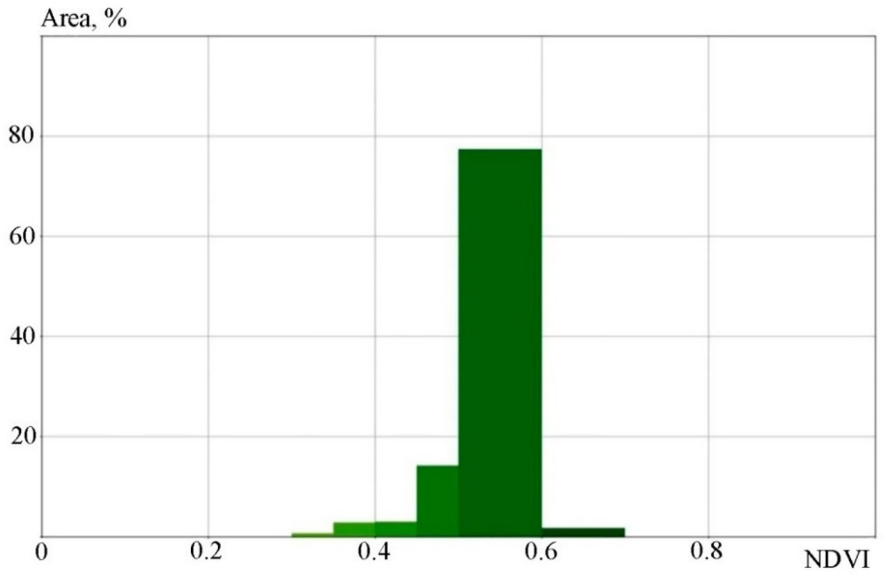

Fig. 2. Distribution of vegetation in pasture No. 1 depending on the NDVI.

Stunted vegetation areas exhibit low NDVI values. The obtained data were used to construct a histogram showing the distribution of vegetation depending on the NDVI value required to identify pasture areas suitable for livestock to graze on [47, 6, 26, 13].

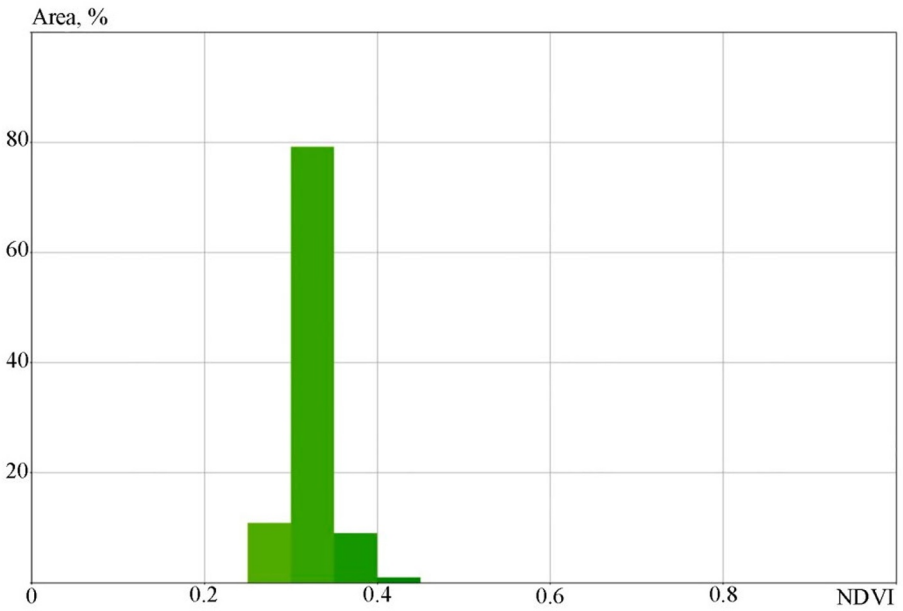

Fig. 3. Distribution of vegetation in pasture No. 2 depending on the NDVI.

Haoyu Jin et al. note that the main factor affecting the NDVI in most areas of China is surface soil moisture (SSM), followed by temperature, whereas in arid areas, the primary

influencing factors include profile soil moisture (PSM) and root zone soil moisture (RZSM) [19].

However, it should be taken into account that NDVI time series contain a lot of contamination due to atmospheric phenomena, cloud cover, sensor failure, etc. It is of utmost importance to eliminate noise prior to any further procedures [39, 35, 44, 16].

In this work, we studied two pastures (47.5 ha each) used for Jalgin Merino sheep to graze on. The presented graphs indicate that 78% (35.6 ha) of the vegetation area in the pastures under study has the NDVI: 0.5 to 0.6 – pasture No. 1; 0.3 to 0.35 – pasture No. 2.

Since the considered pasture areas are located in an arid region of Stavropol Territory, NDMI and SAVI data are of interest here (Figs. 4 and 5).

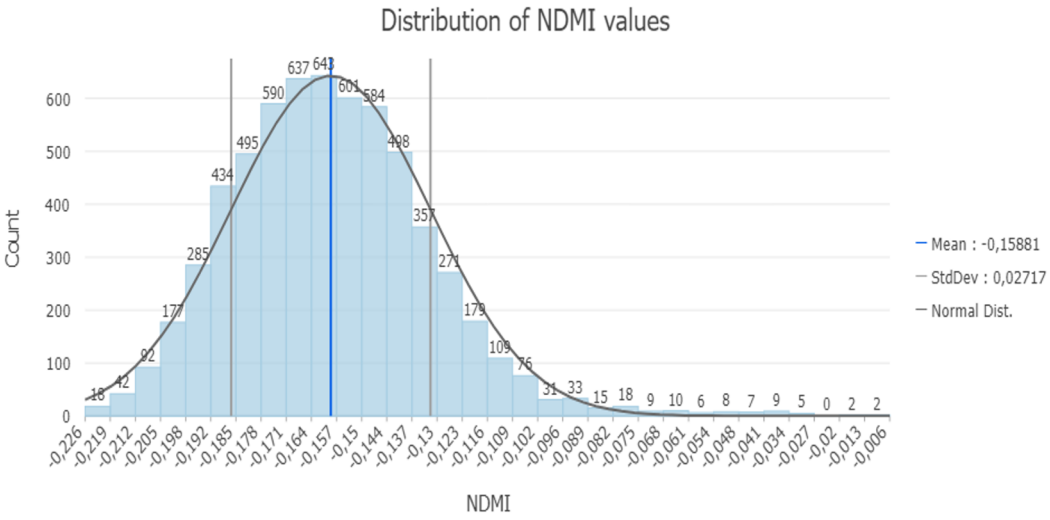

Fig. 4. Distribution of NDMI values.

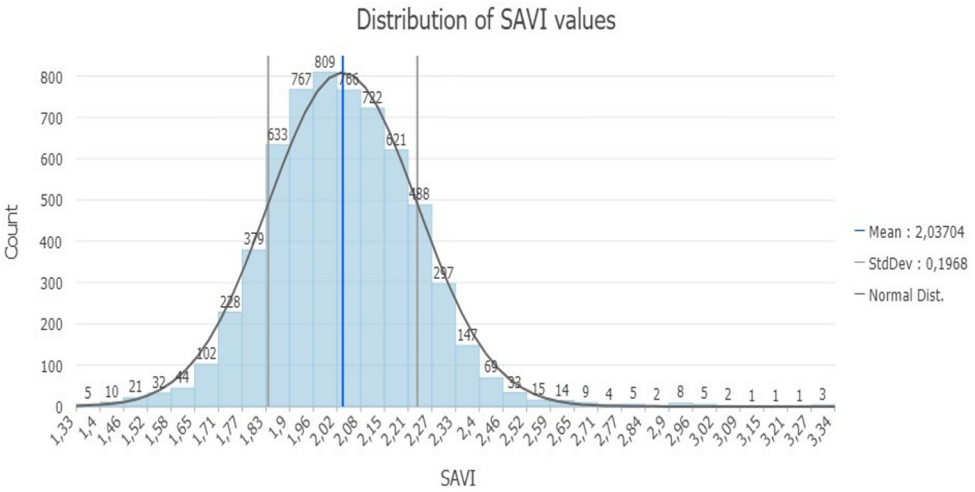

Fig. 5. Distribution of SAVI values

The paper examines the representativeness of the main indices, such as NDVI, SAVI, and NDMI, as well as pasture productivity indicators. The figures presented above show

that all corresponding distributions of index values according to the pixels of a raster image tend to be close to normal, varying in sample means and standard deviations.

Figure 6 displays normal distributions exhibiting the parameters of the corresponding index distributions.

In order to compare data obtained using remote and contact methods, forage samples selected from the pastures under study were subjected to a chemical analysis.

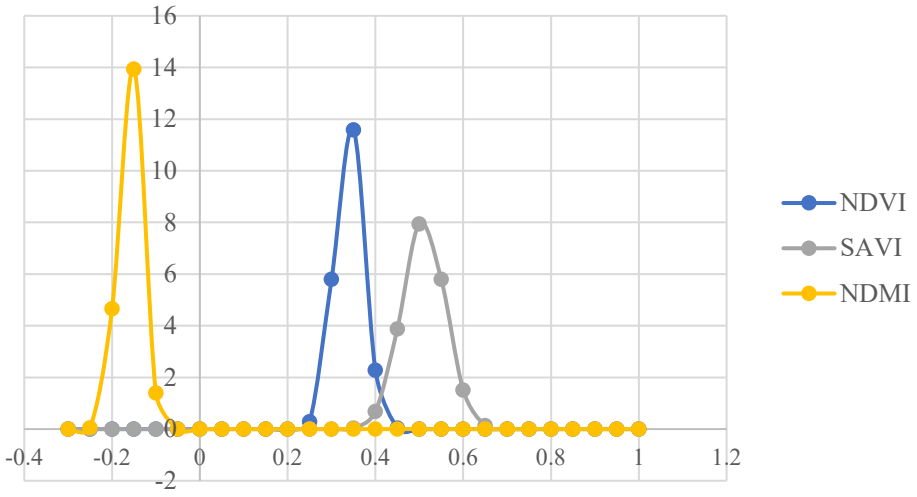

Fig. 6. Distributions of the main indices.

Further research will be aimed at establishing a statistical relationship over time between the distribution parameters of the specified indices and pasture productivity indicators. The study of this relationship will enable construction of the statistical regression models of pasture productivity indicators, which can be used as a basis for clustering pastures on the map.

3.3 Chemical composition of pasture forages

Once grass was mowed and weighed, ten samples were collected from each considered pasture and placed in a polyethylene bag having clips, which were then combined to obtain an average value and spread out evenly. An average grass sample (small tufts from over 20 spots) was collected from it. Labeled samples were placed in specialized containers in an amount of 1 kg. Then the samples were promptly sent to the laboratory.

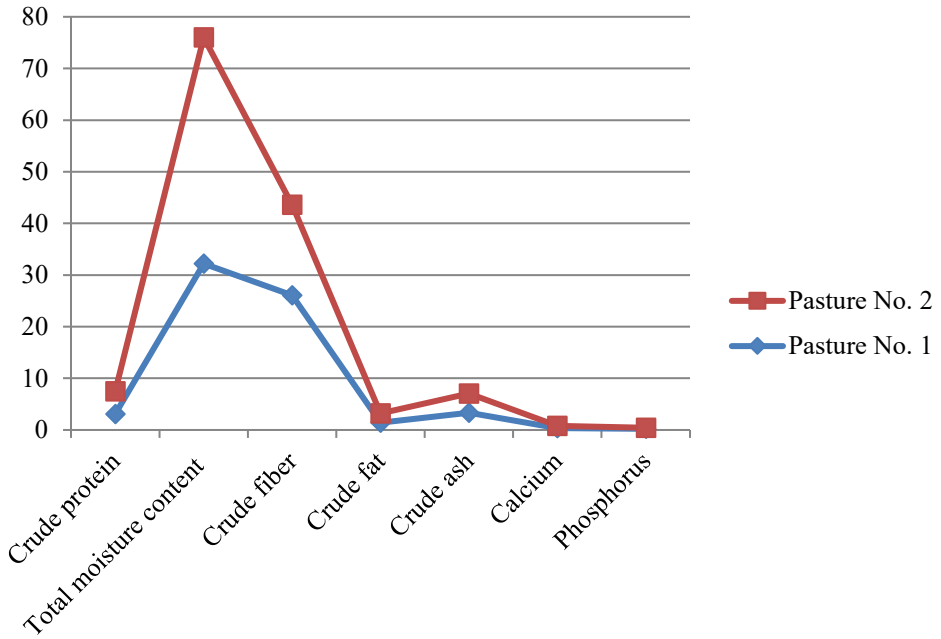

Fig. 7. Nutritional value of pasture forages, %

As compared to forages from pasture No. 2, forages from pasture No. 1 have a higher crude protein content (by 1.65), total moisture content (by 11.48), crude fat (by 0.36), crude ash (by 0.48), calcium (by 0.02), phosphorus (by 0.03), while their crude fiber content is lower by 7.65.

Thus, the pasture forages in group No. 1 exhibit higher values of crude protein, total moisture content, crude fat, crude ash, and calcium, on average, exceeding those of group No. 2 by 5.0–57.0%. Therefore, an inverse correlation is observed between the vegetation index and the content of crude fiber and phosphorus.

Animal feed, specifically protein feed, cannot be regarded as nutritious without considering the role of individual amino acids. Even in the case of a positive protein balance, an animal's body may be deficient in protein. This deficiency may be attributed to the poor absorption of individual interrelated amino acids; the lack or excess of one amino acid can lead to the deficiency of another amino acid. Therefore, it was decided to study the amino acid composition of pasture forages during their contact evaluation, while analyzing the obtained data against the vegetation index.

Figure 9 presents the results of studying the amino acid composition of pasture forages along with the vegetation index observed when rearing Jalgin Merino sheep in the steppes of Stavropol Territory.

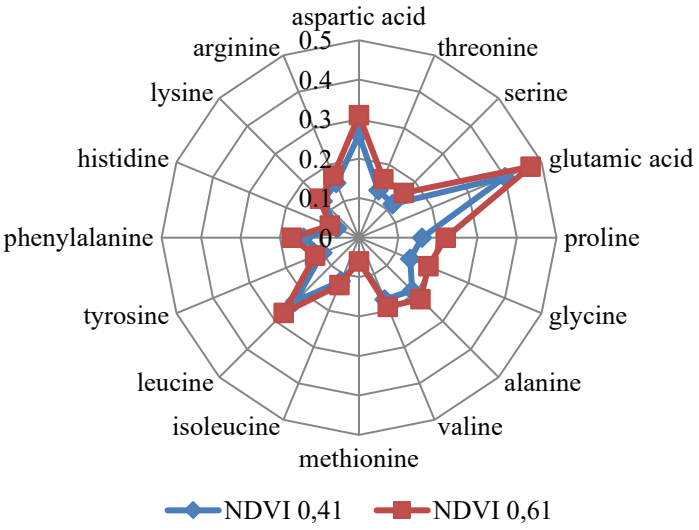

Fig. 8. Amino acid composition of pasture forages, %

According to the data obtained for the second group whose vegetation index of pasture forages is higher, its content of essential and nonessential amino acids exceeds that of the first group by an average of 7.7–47.6%. Thus, the content of aspartic acid (Asp) in the second group (NDVI of 0.61) exceeds that in the first group (NDVI of 0.41) by 47.6%. A similar situation can be observed for other amino acids: threonine (Thr) – by 23.1%; serine (Ser) – by 33.3%; glutamic acid (Glu) – by 17.5%; proline (Pro) – by 37.5%; glycine (Gly) – by 35.7%; alanine (Ala) – by 24.4%; valine (Val) – by 11.8%; isoleucine (Ile) – by 8.3%; leucine (Leu) – by 17.4%; tyrosine (Tyr) – by 20.0%; phenylalanine (Phe) – by 21.4%; histidine (His) – by 33.3%; lysine (Lys) – by 7.7%; arginine (Arg) – by 13.3%.

By taking into account the actual data on the state of pasture vegetation obtained during histogram construction, as well as by combining remote methods for estimating the vegetation index and in-depth nutritional analysis of forages, it becomes possible to optimize the use of pasture plots, which in turn enables an additional 11.06 % increase in daily live weight gain in young merino sheep. Thus, the level of daily live weight gain in the experimental control group formed employing traditional selection procedures amounts to 145 ± 5 g, while the optimization, which allows areas characterized by the highest NDVI value to be used, yields a daily live weight gain of 161 ± 6 g in the young sheep from the experimental group.

The optimized use of pasture areas acquires particular importance in summer and autumn, when the grazing season, in the classical sense, is no longer possible in the arid climate of southern Russia under present-day conditions due to excessively plowed (up to 80%) agricultural land.

The 3D modeling of a pasture plot enables remote estimation of surface topography affecting moisture accumulation, as well as the accumulation of forage and pasture plant biomass. The 3D remote modeling can be employed in combination with NDVI estimation to make production plans for the use of agricultural plots, including for grazing animals.

4 Discussion

The study results indicate that livestock should graze on pasture plots having a vegetation index of at least 0.5. These findings are also confirmed in the study by Md Lokman Hossain and Jianfeng Li, according to which the NDVI varied considerably across regions. As compared to the "base-mean," the NDVI index was significantly higher in a moderately humid region, while in a temperate dry steppe region, a considerably lower NDVI value was observed. Although the NDVI index exhibited a wide variation across plots in cold steppe, no significant variations were observed relative to the base-mean. The following mean NDVI values were obtained for the regions: 0.60 in cold steppe; 0.75 in a moderately humid region; 0.46 in temperate dry steppe [31]. Thus, humid regions exhibit the highest vegetation indices, which corresponds to the data obtained in this study.

X. Chuai et al. describe in their study a relationship between changes in the NDVI index and climatic factors, as well as the potential influence of human activity on the observed changes in the NDVI index in the north of the Loess Plateau. The spatial distribution of the annual NDVI maximum in the north of the Loess Plateau exhibits distinct nonuniformity. It is noted that the NDVI parameters gradually decrease from east to west, while the annual NDVI maximum amounts to 0.44, increasing at a rate of 0.09 in a decade [8, 23, 31].

In the work by Qing Lu et al. precipitation was found to have a greater effect on the NDVI parameters than temperature in Inner Mongolia. The coefficients of correlation between the NDVI values and annual precipitation in the western, central, and eastern districts amounted to about 0.5, which indicates an average correlation, with the lowest correlations observed in the eastern district. The correlations between the NDVI parameters and temperature in Inner Mongolia were generally negative; only some areas in the western region exhibited a positive correlation, passing the significance test [25].

A higher NDVI suggests better vegetation productivity in pasture areas. The obtained data are also consistent with the study by Haoyu Jin et al., which found that more productive vegetation exhibits lower resilience than less productive vegetation (i.e., temperate dry steppe indicates lower NDVI) [19].

Thus, the application of various remote methods for monitoring pasture plots proves to be the most efficient way to use data derived from space satellite systems. Through the simultaneous observation of large pasture plots, it becomes possible to analytically select those that are characterized by the best NDVI parameters, as well as other spectral indices. Systematic observations relying on the interpretation of archived satellite images enable estimation of moisture accumulation in pasture plots throughout the year, including winter. A specific feature of pastoralism consists in organizing the grazing of animals on the basis of the cheapest pasture forages, which can be used by animals for a relatively short period of 5–7 months during the vegetation of various grasses and legumes (at their ratio of 75:25 as established in this study). The presence of legumes having a higher concentration of plant protein generally results in higher live weight gains as compared to plots primarily comprising grasses.

5 Conclusions

1. The application of remote monitoring on the basis of a satellite service enables the construction of 3D mathematical models of agricultural lands, resulting in a more efficient use of pastures.

2. The studies carried out using contact methods confirmed the positive relationship between the vegetation index obtained via the remote method and the nutritional value of forages.
3. The optimization of pasture area selection provides an additional 11.06% ($p<0.05$) increase in live weight gain in young merino sheep.

Acknowledgements

The study was funded by the Ministry of Science and Higher Education and the Ministry of Agriculture of the Russian Federation under the development project Agroinnopolis – 2030 for 2021–2030 of the Stavropol State University. The study was supported by a grant from the Russian Science Foundation № 22-26-20112, https://rscf.ru/project/22-26-20112/.

Compliance with ethics guidelines

Sergey Oleinik, Valentin Skripkin, Tatyana Lesnyak, and Dmitriy Litvin have no relevant financial or non-financial interests to disclose. This article does not include data on studies involving human participants conducted by any of the authors.

References

1. M. Arza-García, M. Gil-Docampo, and J. Ortiz-Sanz, J. Cult. Herit., **38**, 195–203 (2019) doi: 10.1016/j.culher.2019.01.001.
2. S. Backhaus, J. Kreyling, K. Grant, C. Beierkuhnlein, J. Walter, and A. Jentsch, Ecosystems, **17(6)**, 1068–1081 (2014) doi: 10.1007/s10021-014-9781-5.
3. B.D.S. Barbosa, G.A.S. Ferraz, L.M. Gonçalves, D.B. Marin, D.T. Maciel, P.F.P. Ferraz and G. Rossi, Agronomy Research, **17(22)**, 349-357 (2019) doi: 10.15159/ar.19.119.
4. K. Benjmel, F. Amraoui, S. Boutaleb, M. Ouchchen, A. Tahiri, and A. Touab, Water, **12 (2)**, 471 (2020) doi: 10.3390/w12020471.
5. L. Castillo-Villamor et al. Int. J. Appl. Earth Obs. Geoinf., **104**, 102535 (2021) doi: 10.1016/j.jag.2021.102535.
6. R. Catorci, L. Lulli, M. Malatesta, F. Tavoloni, and M. Tardella, Agric. Ecosyst. Environ., **314**, 107372 (2021) doi: 10.1016/j.agee.2021.107372.
7. H. Chu, S. Venevsky, C. Wu, and M. Wang, Sci. Total Environ., **650**, 2051–2062 (2016) doi: 10.1016/j.scitotenv.2018.09.115.
8. X. W. Chuai, X. J. Huang, W. J. Wang, and G. Bao, Int. J. Climatol., **33 (7)**, 1696–1706 (2013) doi: 10.1002/joc.3543.
9. J. P. Dash, M. S. Watt, G. D. Pearse, M. Heaphy, and H. S. Dungey, ISPRS J. Photogramm. Remote Sens., **131**, 1–14 (2017) doi: 10.1016/j.isprsjprs.2017.07.007.
10. W. De Keersmaecker et al., J. Appl. Ecol., **53 (2)**, 430–439 (2016) doi: 10.1111/1365-2664.12595.
11. C. Gang et al., Environ. Earth Sci., **72 (11)**, 4273–4282 (2014) doi: 10.1007/s12665-014-3322-6.
12. Y. Gül, *Türkiye Jeol. Bülteni, Geol. Bull. Turkey* (2019) doi: 10.25288/tjb.519506.

13. R.R. Fern, E.A. Foxley, A. Bruno, and M. L. Morrison, Ecol. Indic., **94**, 16–21 (2018) doi: 10.1016/j.ecolind.2018.06.029.
14. Y. Furukawa and J. Ponce, *Accurate, Dense, and Robust Multi-View Stereopsis,* 2007 IEEE Conference on Computer Vision and Pattern Recognition, 1–8 (2007) doi: 10.1109/CVPR.2007.383246.
15. M.L. Hossain and J. Li, Glob. Ecol. Conserv., **30**, e01768 (2021) doi: 10.1016/j.gecco.2021.e01768.
16. T. Hua, X. Wang, C. Zhang, L. Lang, and H. Li, L. Degrad. Dev., **28 (7)**, 1913–1921 (2017) doi: 10.1002/ldr.2709.
17. G. Idoje, T. Dagiuklas, and M. Iqbal, Comput. Electr. Eng., **92**, 107104 (2021) doi: 10.1016/j.compeleceng.2021.10 7104.
18. J. Iglhaut, C. Cabo, S. Puliti, L. Piermattei, J. O'Connor, and J. Rosette, Curr. For. Reports, **5 (3)**, 155–168 (2019) doi: 10.1007/s40725-019-00094-3.
19. H. Jin et al. J. Hydrol., **603**, 127129 (2021) doi: 10.1016/j.jhydrol.2021.127129.
20. D. Kachamba, H. Ørka, T. Gobakken, T. Eid, and W. Mwase, Remote Sens., **8 (11)**, 968 (2016) doi: 10.3390/rs8110968.
21. S. Li, L. Xu, Y. Jing, H. Yin, X. Li, and X. Guan, Int. J. Appl. Earth Obs. Geoinf., **105**, 102640 (2021) doi: 10.1016/j.jag.2021.102640.
22. Y. Li et al., Sustainability, **11 (5)**, 1281 (2019) doi: 10.3390/su11051281.
23. X. Li, Y. Li, A. Chen, M. Gao, I. J. Slette, and S. Piao, Agric. For. Meteorol., **269–270**, 239–248 (2019) doi: 10.1016/j.agrformet.2019.01.036.
24. Y. Liu, H. Liu, L. Wang, M. Xu, S. Cohen, and K. Liu, J. Hydrol. **603**, 126876 (2021) doi: 10.1016/j.jhydrol.2021.126876.
25. Q. Lu, D. Zhao, S. Wu, E. Dai, and J. Gao, Theor. Appl. Climatol., **135**, 3–4 (2019) doi: 10.1007/s00704-018-2614-2.
26. M.M. McIntosh, J. L. Holechek, S.A. Spiegal, A.F. Cibils, and R.E. Estell, Rangel. Ecol. Manag., **72 (6)**, 976–987 (2019) doi: 10.1016/j.rama.2019.06.002.
27. S. Nebiker, N. Lack, M. Abächerli, and S. Läderach, Int. Arch. Photogramm. Remote Sens. Spat. Inf. Sci., **XLI-B1**, 963–970 (2016) doi: 10.5194/isprsarchives-XLI-B1-963-2016.
28. J.M. Peña, J. Torres-Sánchez, A. I. de Castro, M. Kelly, and F. López-Granados, PLoS One, **8(10)**, e77151 (2013) doi: 10.1371/journal.pone.0077151.
29. M. Pepe and D. Costantino, *UAV Photogrammetry and 3D Modelling of Complex Architecture for Maintenance Purposes: the Case Study of the Masonry Bridge on the Sele River*, Italy. Period. Polytech. Civ. Eng. (2020) doi: 10.3311/PPci.16398.
30. M. Pepe, D. Costantino, V. S. Alfio, and N. Zannotti, Geogr. Tech., **Special Issue**, 1–14 (2020) doi: 10.21163/GT_2021.163.01.
31. J. Pinzon and C. Tucker, Remote Sens., **6 (8)**, 6929–6960 (2014) doi: 10.3390/rs6086929.
32. S. Piao, A. Mohammat, J. Fang, Q. Cai, and J. Feng, *Glob. Environ. Chang.*, **16 (4)**, 340–348 (2006) doi: 10.1016/j.gloenv cha.2006.02.002.
33. S. Sankaran et al., Eur. J. Agron., **70**, 112–123 (2015) doi: 10.1016/j.eja.2015.07.004.
34. Sinde-González et al., Int. J. Appl. Earth Obs. Geoinf., **101**, 102355 (2021) doi: 10.1016/j.jag.2021.102355.

35. H. Sun et al*., Vegetation Change and Its Response to Climate Change in Yunnan Province*, (China, Adv. Meteorol*.,* 2021) 1–20. doi: 10.1155/2021/8857589.
36. D. Thakur, S.K. Bartarya, and H.C. Nainwal, Environ. Earth Sci., **77 (10)**, 368 (2018) doi: 10.1007/s12665-018-7552-x.
37. P.S. Thenkabail, R.B. Smith, and E. De Pauw, Remote Sens. Environ., **71(2)**, 158–182 (2000) doi: 10.1016/S0034-4257(99)00067-X.
38. S.M. Vicente-Serrano, J.J. Camarero, and C. Azorin-Molina, Glob. Ecol. Biogeogr. **23(9)**, 1019–1030 (2014) doi: 10.1111/geb.12183.
39. Z. Wang et al., Ecol. Inform., **33**, 32–44 (2016) doi: 10.1016/j.ecoinf.2016.03.006.
40. W. Yao, X. Wang, Y. Lan, and J. Jin, Front. Agric. Sci. Eng. (2018) doi: 10.15302/J-FASE-2018232.
41. J. Yao et al., Theor. Appl. Climatol., **131**, 3–4, 1503–1515 (2018) doi: 10.1007/s00704-017-2058-0.
42. Y. Zhang and N. Zhang, Front. Agric. Sci. Eng. (2018) doi: 10.15302/J-FASE-2018242.
43. Q. Zhang, D. Kong, V. P. Singh, and P. Shi, Glob. Planet. Change, **152**, 1–11 (2017) doi: 10.1016/j.gloplacha.2017.02.008.
44. Zhao, Q. Yu, L. Feng, A. Zhang, and T. Pei, J. Environ. Manage., **261**, 110214 (2020) doi: 10.1016/j.jenvman.2020.110214.
45. C. Zhao and M. Li, Front. Agric. Sci. Eng., **5(4)**, 391–392 (2018) doi: 10.15302/J-FASE-2018246.
46. Q. Zhou, Q. Yu, J. Liu, W. Wu, and H. Tang, J. Integr. Agric., **16 (2),** 242–251 (2017) doi: 10.1016/S2095-3119(16)61479-X.
47. M. Zhumanova, C. Mönnig, C. Hergarten, D. Darr, and N. Wrage-Mönnig, Ecol. Indic., **95**, 527–543 (2018) doi: 10.1016/j.ecolind.2018.07.060.